

UNCLASSIFIED



L A 46

**PUBLICLY RELEASABLE**

Per B. Latinius, FSS-16 Date: no date  
By J. DeB, CIC-14 Date: 3-11-96



January 4, 1944

This document contains 34 pages

A COMPARISON OF BORON AND 25 FISSION CROSS-SECTIONS  
FOR NEUTRONS OF ENERGIES FROM THERMAL TO 3 MEV

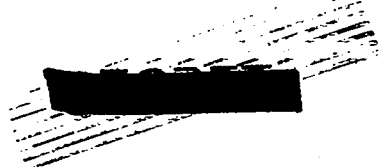
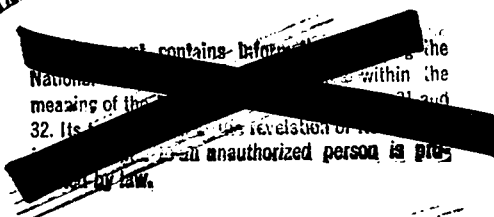
WORK DONE BY:

- C. L. Bailey
- J. E. Blair
- W. C. Bright
- D. H. Frisch
- K. Greisen
- A. O. Hanson
- J. E. Hush
- E. J. Konopinski
- R. Krohn
- J. L. McKibben
- R. Perry
- H. R. Richards
- R. F. Taschek
- C. M. Turner
- J. H. Williams

REPORT WRITTEN BY:

- C. L. Bailey
- A. O. Hanson
- E. J. Konopinski

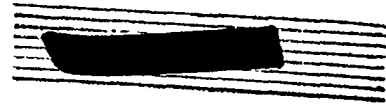
Classification changed to UNCLASSIFIED  
by authority of the U. S. Atomic Energy Commission.  
Per H. Z. Carroll 3-22-56  
By R. F. Marking 4-5-56  
By REPORT LIBRARY



UNCLASSIFIED

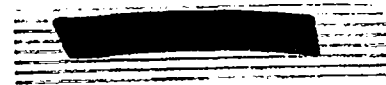
UNCLASSIFIED

-2-

ABSTRACT

A comparison of the  $^{25}\text{F}$  fission cross-section to that of boron for neutrons of energies ranging from thermal to a few kilovolts was made by comparing the counting rates from a  $^{25}\text{F}$  and a boron film when shielded by various amounts of boron absorber. An increase in  $\sigma_{25} \cdot \sqrt{E}$  by a factor of 3.3 is found to occur in the region of 2 to 200 ev.

A comparison of  $\sigma_B$  and  $\sigma_{25}$  for neutrons with energies from 0.15 to 1.5 Mev gives a fairly good picture of  $\sigma_B$  in this energy range. A resonance in  $\sigma_B \cdot \sqrt{E}$  is found at about 0.25 Mev. The maximum value of this quantity is from 2 to 3 times that at thermal values.



UNCLASSIFIED

**UNCLASSIFIED**  

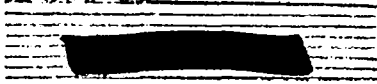

-5-

A COMPARISON OF BORON AND 25 FISSION CROSS-SECTIONS FOR NEUTRONS  
OF ENERGIES FROM THERMAL TO 3 MEV

INTRODUCTION

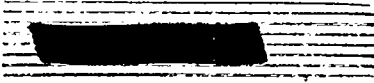
Measurements on the neutron capture cross-section of boron have been made by R.F. Bacher, G.P. Baker, and B.D. McDaniel (C-25) using the modulated beam method. Their measurements were carried up to approximately 50 ev and it was found that the boron absorption cross-section obeyed the  $1/v$  law up to that energy. Their results gave a value of 708 barns for the absorption cross-section for thermal neutrons (0.025 ev). Measurements made at Chicago confirm this value for the thermal cross-section.

Measurements of the 25 fission cross-section for thermal neutrons have also been made at Chicago which gave a value of 645 barns (CP-1088). No extensive measurements have been made on the behavior of  $\sigma_{25}$  as a function of energy in the low energy region. Measurements of the 25 fission cross-section have been made in more detail for neutrons of energies from 0.15 to 1.9 Mev by the Wisconsin group. (See A.O. Hanson CP-618, or LA Handbook LA-11) The values at high energies indicate a value which is approximately 12 times that which would be obtained by extrapolating the thermal cross-section to these energies on the assumption that the  $1/v$  law is valid throughout the entire energy range.

**UNCLASSIFIED**

The only previous measurement of the boron cross-section for high energy neutrons is one made by N.P. Heydenburg and R.C. Meyer (GF-605). They found a value for 0.6 Mev neutrons which was about twice that expected from the  $1/v$  law.

In the absence of any further experimental evidence it was felt that the boron cross-section would obey the  $1/v$  law quite accurately for neutrons of energies up to several kev. Since there was such a large break in the behavior of the 25 fission cross-section in the region between thermal neutrons and 0.1 Mev neutrons, it was suggested by E. Teller that a good deal of information could be obtained by comparing the counting rates from a 25 and a boron film when shielded by suitable amounts of boron. For such an experiment it is desirable to have a source of neutrons which would give an approximately constant counting rate per unit logarithmic energy interval in the region from thermal energies to several kilovolts. It was found, however, that the calculation of the expected spectrum from such a source was very sensitive to the amount of slowing-down material used as well as to the initial energy spectrum of the neutrons from the source. However, taking the differences in the counting rates when the amount of boron absorber is increased the effect of the uncertainty in the neutron spectrum is reduced. The details of this experiment as carried out will be discussed under a separate heading.

Another experiment designed to give information about the boron cross-section was the comparison of the boron and 25 cross-sections in the region where the 25 cross-section has been studied. This experiment required 

only a direct comparison of the counting rates in the boron and 25 chambers when placed in the same flux of high energy neutrons. The main ambiguity in this experiment is the uncertainty in the absolute values of the 25 cross-section.

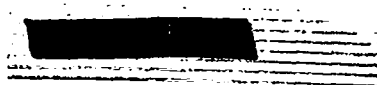
### TELLER EXPERIMENT

#### Experimental Arrangement

The experimental arrangement for determining the ratio  $\sigma_B/\sigma_{25}$  at low energies is shown in Fig. 1a. In outline the method is to place a boron  $\alpha$ -particle detector and a 25 fission detector in the same neutron flux, change the minimum energy of the neutrons striking the detectors by placing suitable amounts of boron carbide around the detectors and observe the counting rates in the two detectors as a function of the absorber thickness.

Neutrons were obtained from a thick lithium target bombarded by 1.93 Mev protons from the short electrostatic generator in W. This meant that the maximum energy of the neutrons emitted at  $0^\circ$  was about 170 kev and of those emitted at  $90^\circ$  about 25 kev. The average energy including neutrons emitted at all angles from a thick target was computed to be about 5 kev. The target was surrounded by a paraffin sphere having a radius of 3.5 cm, or alternatively by a carbon sphere having a radius of 12 cm.

The detector samples consisted of thin films of boron and 25 on platinum foils. The 25 foils had a density of less than 40 micrograms of 25 per  $\text{cm}^2$ , and the boron film had a considerably lower density so there could be no appreciable shielding due to absorption of neutrons in the foils. These



foils were mounted on opposite sides of the common high voltage electrode in the double ionization chamber as shown in Fig. 1b. This electrode was made of aluminum (center portion 1/32 inch thick) to be certain that there was no absorption and hence no difference in the neutron flux on the two sides. To increase the intensity a second 25 foil was placed on the opposite electrode of the 25 chamber. The chambers were operated with air at atmospheric pressure and with a collecting voltage of about 1000 volts per cm. The double chamber was surrounded by a large shield can filled with boron carbide, as shown in Fig. 1a. The energy-limiting absorbers, made of brass pillboxes filled with boron carbide ( $B_4C$ ), were fitted into the open end of the can. To minimize errors due to scattering, the absorbers were placed so that their centers were at a constant distance from the ionization chambers. With the exception of one run, a cadmium sheet was left in when  $B_4C$  absorbers were added. A table giving the data on the absorbers used is found below.

TABLE I. TABLE OF ABSORBERS.

No.	$l$ gms/cm <sup>2</sup>	Transmitted, $E_0$ Approx. Min. Energy
1	0.26	1.5 ev
2	0.49	6.0 ev
3	1.00	25 ev
4	2.00	100 ev
5	4.00	400 ev

The energy limit given in the last column is the energy at which the absorber

-7-

transmits  $1/e$  of the neutrons. This energy is approximately  $E_0 = 25l^2$  volts, if  $l$  is in  $\text{gm/cm}^2$ .

The counting rates (B and F) in the boron and the 25 chamber were observed simultaneously as a function of absorber thickness. The flux was monitored by a boron carbide lined chamber placed outside as shown in Fig. 1a. Runs were taken with the paraffin sphere with the detectors at  $0^\circ$  and at  $80^\circ$ , and with a graphite sphere at  $90^\circ$ . The last run with paraffin and the detectors at  $80^\circ$  was most carefully done. (See Fig. 4.) In this run sufficiently many counts were observed so that statistical errors were reduced to about 2 percent.

### Results

The results of several runs are given in Table II. The second and third groups of columns show the ratios of boron counts (B) and 25 counts (F) to the monitor count (M) for each absorber indicated in the first column. Since different monitors were used for the different runs, numerical comparisons between the B and F data from different runs are not possible. Two runs made at  $80^\circ$  are included to give an indication of the consistency of the data.

The third group of columns shows the boron to 25 fission ratio as a function of absorber thickness. As more of the slower neutrons are cut out by successive additions of absorber, the B/F ratio is seen to fall, showing that the 25 fission does not follow the  $1/v$  law as is expected of boron. Instead, the faster neutrons show themselves to be relatively more efficient in causing 25 fission. A somewhat more quantitative description of this trend is shown by the last group of columns. These give the ratios of the

changes in boron and 25 counts caused by successive additions of absorber. Thus is obtained the effect of neutrons too energetic to be stopped by one absorber but stopped by the next thicker one. If one assumes that such neutrons have a mean energy which is an average of the transmission limits as given in the Table of Absorbers (I), one can assign  $E/F$  values to various neutron energies. Results of such an assignment of energy values are shown in Figs. 3 and 4; the latter figure is based on the run regarded as the most reliable. Recalling  $\sigma_y \sim 1/v$ , one sees from the graphs that  $\sigma_{25-V}$  increases by a factor 3 or so between neutron energies of some 2 to 200 ev. Of course, this is only a small part of the expected rise by a factor 12 which presumably should take place before energies in the neighborhood of several hundred kilovolts are reached.



TABLE II.

Ascorbar	R/H			F/H			I/F			$\frac{\Delta(R/H)}{\Delta(F/H)}$			
	Par. 80°	Par. 0°	Carbon 90°	Par. 80°	Par. 0°	Carbon 90°	Par. 80°	Par. 0°	Carbon 90°	Par. 80		Par. 0°	Carbon 90°
										Cd	No Cd		
None	129.2	48.7	4.63	60.6	22.9	3.96	2.13	2.13	1.17				
	129.2			60.6			2.14						
										2.29		2.33	1.90
										2.28			
Cd only	19.9	8.50	3.19	12.8	5.63	3.20	1.55	1.52	.996				
	21.3			13.5			1.60					2.28	
#1	14.7		2.45	10.5		2.75	1.41		.895				
										2.32		2.66	1.70
										2.86			
Cd + #1	10.4	4.70	2.24	8.75	4.20	2.64	1.19	1.12	.850				
	11.0			9.70			1.13					2.82	
#2	9.20			8.55			1.08						
										2.30		2.13	1.46
										2.00			

APPROVED FOR PUBLIC RELEASE

TABLE II (cont'd)

Absorber	B/M			F/M			B/F			$\frac{\Delta(B/H)}{\Delta(F/H)}$			
	Par. 30°	Par 0°	Carbon 90°	Par. 80°	Par. 0°	Carbon 90°	Par. 80°	Par. 0°	Carbon 90°	Par. 80°		Par. 0°	Carbon 90°
										Cd	No Cd		
Cd + #2	7.75	3.38	1.96	7.61	3.58	2.38	1.01	.940	.780				
	7.65			7.95			.962					1.34	
Cd + #1 + #2		2.44			2.88			.855				1.59	
#3	5.56			6.26			.890						
										1.56		2.60	.790
										1.12			
Cd + #3	6.14	2.13	1.42	5.94	2.78	1.82	.870	.794	.780				
	4.57			5.20			.870						
												.92	
Cd + #2 + #3		1.39			1.92			.727					
										1.07		.55	.96
										.88			
Cd + #4	2.60	1.26	1.01	3.55	1.72	1.40	.730	.725	.720				
	2.88			3.28			.883						
												.97	

TABLE II (cont'd)

Absorber	B/H			F/M			B/F			$\frac{\Delta(B/H)}{\Delta(F/M)}$			
	Par. 80°	Par. 0°	Carbon 90°	Par. 80°	Par. 0°	Carbon 90°	Par. 80°	Par. 0°	Carbon 90°	Par. 80° Cd	Par. 80° NoCd	Par. 0°	Carbon 90°
#5	1.56			2.15			.725						
										.72		.87	.7
Cd + #5	1.52	.662	.580	2.06	1.03	.84	.74	.665	.694				
												.61	
Cd + #4 + #5		.398			.596			.666					
										.77			.8
Cd + #1 + #5	.55		.314	.20		.522	.70		.70				
											.50		
8.5 gm/cm <sup>2</sup>	2.78			4.60			.66						

APPROVED FOR PUBLIC RELEASE

APPROVED FOR PUBLIC RELEASE

### Analysis of Results

Perhaps the results obtained from the rough analysis so far presented are all that one should expect from this relatively simple experiment. However, a somewhat more detailed analysis may help to circumvent some of the criticisms which might be made. It is obvious that each point in Figs. 3 and 4 represents a resultant of a wide group of neutron energies. Moreover the energy limits of the group depend on the intensity with which these energies are represented in the neutron spectrum employed. One can hope to remove some of the ambiguity through some knowledge of the distribution in energy of the neutrons.

One may first attempt to compute the spectrum to be expected under the conditions of the experiment. As a matter of fact, such a computation was carried out in order to decide what experimental conditions to use. It is straightforward to show that the number of neutrons in the energy range  $dE_n$  from a thick target of Li bombarded by protons is proportional to:

$$I dE_n = dE_n \int_{E_1}^{E_2} Y(\theta, E_p) \frac{d(\cos\theta)}{E_n} dE_p$$

$E_p$  is the proton energy in the reaction,  $E_1$  being its threshold value (1.86 MV) and  $E_2$  the bombardment energy possessed by all protons before their slowing in the lithium target.  $Y$  is the yield curve of the Li (p,n) reaction. It was assumed to be the product of two factors; one depending on proton energy only and given in the I. A Handbook; the other depending only on  $\theta$ , the angle of neutron emission in the center-of-mass system. Curves for the latter factor given in a report by Benedict and Hanson (CF-617) led to

$$Y \sim 1 - 3.77 \cos\theta + 4.61 \cos^2\theta$$

for the angle dependence. The last factor in the integrand is found easily from the consideration of energy and momentum conservation in the reaction, which gives

$$\cos\theta = \frac{E_n - (25/32) E_p + (1.42 \text{ MV})}{(7/32) E_p \sqrt{1 - (1.86 \text{ MV}/E_p)}}$$

Numerical integration led to the spectrum shown as I in Fig. 9 for the neutrons from a thick Li target and with  $E_2 = 1.93 \text{ MV}$ .

In order to obtain a greater proportion of the very slow neutrons whose effect was to be explored in the experiment, the source was surrounded by a paraffin sphere. The spectrum resulting from this can be calculated with the usual procedure based on Fermi's slowing-down equation and the assumption of a point source at the center of the paraffin. This procedure cannot be expected to be completely trustworthy for the small amount of paraffin involved in this experiment. The result is shown in Fig. 9. It represents the activity A in a  $1/v$  detector which would be caused by the neutrons in a unit logarithmic energy range, i.e.,  $\int A dE/E$  would be the total activity.

As a check on the computed spectrum one can see whether it leads to the experimentally found boron absorption curve (Fig. 2).

When

$$B = \int_0^{E_{\max}} A e^{-B/\sqrt{E}} (dE/E)$$

was computed it was found to give an absorption curve not quite as steep as the experimental one. Evidently, the actual neutron spectrum has a greater proportion of absorbable slow neutrons. By approximating the above expression for B with

$$B \approx \int_0^{25l^2} A \, dE/E$$

one sees that

$$A \approx \frac{l}{2} \frac{\partial B}{\partial l}$$

so that in this approximation the "activity" spectrum can be obtained from the boron absorption curve by differentiation. This not very accurate procedure yielded the curve shown in Fig. 9. It supports the criticism of the first computed spectrum in that it gives greater weight to the more absorbable, intermediate-energy neutrons. The excess of very slow neutrons in the first spectrum are presumably entirely stopped in the first layers of boron absorber and so contribute nothing to the variation of the absorption curve at greater thicknesses. The new spectrum,  $l \, \partial B / \partial l$ , was found to lead to an absorption curve more nearly in agreement with the experiment than did the first spectrum. However, using this new spectrum for further analysis represents no essential improvement on our first procedure which yielded Figs. 3 and 4. The assumptions remain the same: That there is a one-to-one correspondence between neutron energy and boron thickness as given by  $E \approx 25l^2$ . Thus the inquiry into the spectra has so far netted no more than some additional support, for considering the first procedure fairly sensible.

There remains another procedure, independent of the assumptions involved in the relation  $E \approx 25l^2$ , which may be tried. One can divide the energy range into a few intervals over each of which the "activity"  $A$  is assumed to be constant. The value of the constant in each interval can be treated as an unknown to be evaluated by computing the consequent absorption curve and fitting it to the experimental one. If  $E_1$  and  $E_2$  are the energies delimiting the interval and  $A_{12}$  is the constant "activity" due to neutrons within it, then its contribution to the boron counts through  $l$  gm/cm<sup>2</sup> of absorber is given by:

$$B_{12} = A_{12} \int_{E_1}^{E_2} e^{-5l/\sqrt{E}} dE/E = 2A_{12} \left[ -Ei\left(-\frac{5l}{\sqrt{E_2}}\right) + Ei\left(-\frac{5l}{\sqrt{E_1}}\right) \right]$$

$$\left( = A_{12} \log (E_2/E_1) \text{ for } l = 0 \right)$$

Such contributions from each interval are to be added to obtain the total boron counts  $B$  at a given  $l$ .

The calculation was first carried out for three intervals. The limits of the intervals and the relative values of  $A$  in each, which resulted from fitting to the absorption curve of the 80° data, are given here:

<u>Intervals</u>	<u>A</u>
0.4 (Cd limit) to 25 volts	4.75
25 volts to 400 volts	3.82
400 volts to 10 kev	0.673

The values of  $A$  are plotted as a histogram in Fig. 9. One can hope to make the histogram approach a continuous curve by increasing the number of intervals. One finds, however, that the values of  $A$  are extremely sensitive to variations in the absorption curve and that the sensitivity mounts enormously with the number of intervals. For example, when a four interval analysis was tried on the basis of the experimental absorption curve, a negative  $A$  value was obtained in one of the intervals. This could be remedied by first correcting the experimental curve on the basis of the three-interval analysis; no correction greater than the 1-2 percent statistical fluctuations had to be made. Then the four interval analysis proceeded smoothly with the results:

<u>Interval</u>	<u>A</u>
0.4 to 10 volts	4.93
10 to 63 volts	3.61
63 to 400 volts	2.66
400 to $1.6 \times 10^4$ volts	0.78

This is also plotted in Fig. 9 and shows gratifying agreement with the three-interval analysis. Both indicate that the spectra derived in the preceding paragraphs were not very far wrong. The "doctoring" which was needed to make the four-interval analysis give sensible results indicates that the data were incapable of yielding more than is obtained with the three-interval analysis.

The interval analysis can be used to determine the variation of  $\sigma_{25} \nu$  in the following way. One applies the above procedure to the values of  $F/M$  as a function of  $l$  instead of  $E/M$ , the absorption as detected in B.



-17-

Then in place of A one obtains  $(\sigma_{25}/\sigma_B)A$  and thus  $\sigma_{25 \cdot v}$ . The three-interval analysis thus gave:

<u>Intervals</u>	<u><math>\sigma_{25 \cdot v}/(\sigma_{25 \cdot v})_{\text{thermal}}</math></u>
0.4 to 25 volts	0.57
25 to 400 volts	3.3
400 to $10^4$ volts	3.0

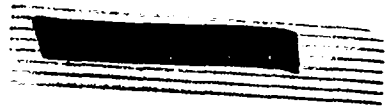
In qualitative agreement with Figs. 3 and 4, this shows that  $\sigma_{25 \cdot v}$  rises by about a factor 3 over the thermal value in the neighborhood of 25-100 volts, staying about constant to some 10 kv. There is some indication of a decrease in  $\sigma_{25 \cdot v}$  below the thermal value between the Cd limit and 25 volts.

It should be mentioned that there may be some error introduced in the above work due to the fact that a small part of the counts observed in the boron chamber were due to nitrogen. This possibility was checked at the conclusion of this experiment and it was found that the background count at the biases used with the boron film removed was approximately 1/6 of the boron counting rate. A run on this background with and without cadmium showed that this background count was reduced in the same ratio as in the run with the boron sample in. Further checks on this point were prevented by a serious breakdown of the electrostatic generator, but it could not change the magnitude of the break by more than about 5 percent.

COMPARISON OF  $\sigma_{25}$  AND  $\sigma_B$  FOR HIGH ENERGY NEUTRONSExperimental Arrangement

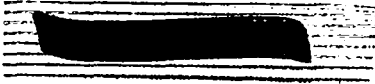
This experiment was carried out using the long electrostatic generator in W. The source of neutrons was again the  $\text{Li}(p,n)$  reaction. The lithium target used had a thickness such as to reduce the energy of the protons by 60 kev. The average energy of the neutrons was taken as that corresponding to a proton energy 30 kev less than the maximum. All detector chambers used with high energy neutrons were placed as close to the target as convenient (3-6 inches) and were covered with cadmium so as to minimize the effect of scattered neutrons.

The experiment, in its simplest form, again consists of comparing the counting rates of the fissions in the 25 chamber and of the  $\alpha$ -particles in a boron chamber. A direct comparison of the cross-sections by simply comparing the counting rates in a comparison chamber such as used in the Teller experiment will not, however, give a correct result where the energy of the neutrons is comparable to the  $Q$  value of the reaction (2.8 Mev). The corrections to be applied to the counting rates from thick and thin boron films were considered and it was found that the corrections would be very large even for neutrons having energies around 0.5 Mev where the difference in the counting rate would be of the order of 50 percent depending on whether the  $\alpha$ -particles counted came out of the foil toward or away from the source of neutrons. These corrections are complicated by the fact that they depend on the bias of the recording instrument, and by the fact that two  $Q$  values



must be considered, one corresponding to leaving the Li nucleus in an excited state, and that counts arising from the Li recoil must also be considered. There is a simplification if really thin films are used in that the average of the counting rates taken with the film turned toward and away from the source gives the correct value. The data taken in this experiment with the thin films were evaluated in this way. The use of such a chamber (Fig. 1b) has the advantage that the ratio of the counting rates observed at high energies can be compared to that at thermal energies (neutrons absorbed by Cd) by simply placing the chamber in the center of a large block of paraffin. In this way the change in the ratio of cross-sections from thermal energies to the higher energies can be measured directly. The ratios measured in this way are shown by the triangular points in Fig. 6. It was unprofitable to use this method with neutrons having an energy greater than 0.4 Mev since the background in the chamber became important and could not be corrected for with any certainty.

To get the variation in the ratio of  $\sigma_B/\sigma_{25}$  at higher energies a gas chamber filled with BF<sub>3</sub> and a 25 fission chamber were used. The use of a gas chamber is particularly advantageous in that either the  $\alpha$ -particle or the Li recoil from the B(n, $\alpha$ )Li reaction will almost always have its complete range in the chamber and hence insure a minimum pulse of about one Mev (the minimum energy of the Li recoil). With this chamber one could set the bias at a point corresponding to about 1 Mev pulses and be certain that all the B(n, $\alpha$ ) reactions were counted and that there would be no confusion due to proton recoils or other reactions occurring in the chamber walls which have a low Q value. It was found that it was necessary to use a collecting voltage



-20-

of about 4000 volts on a chamber such as is shown in Fig. 5 filled with 60 cm  $\text{BF}_3$  in order to get a good plateau in the numbers vs bias curves. The data taken with this chamber is shown on Fig. 6 by X's. In this and the following run the boron chamber and the fission chamber were placed at an angle of  $30^\circ$  to the forward direction. The data from this run seemed reliable up to above 1 Mev but at this point there was no longer a reliable plateau. A second gas chamber was then constructed in an attempt to use higher pressures and higher collecting fields and so increase the length of the plateau. This chamber is the one shown in Fig. 5 and it made possible the use of collecting voltages of more than 6000 volts when the chamber was filled with 15 cm  $\text{BF}_3$  and 60 lbs (gauge) of spectroscopically pure argon. Much of the designing and testing of these chambers was done by J. M. Blair. This chamber when exposed to slow neutrons gave a satisfactory plateau up to a bias point corresponding to 1.5 Mev pulses in the chamber. The results obtained with this chamber are shown as plus signs in Fig. 6. For this run complete bias curves were obtained with and without  $\text{BF}_3$  in the chamber for each point. For the highest energy point the background count amounted to about 30 percent at a bias corresponding to 1 Mev pulses. However, by subtracting the background count satisfactory plateaus were obtained for all points. The origin of the background count is not clear but is presumably from the brass walls of the chamber. It might be pointed out that this last run should have detected any appreciable amount of the  $\text{B}^{10}(n,p)$  reaction which from the mass values should have a Q value of about 0.2 Mev. Its absence is in agreement with expectations that it would be only about one percent as probable as the  $(n,\alpha)$  reaction.

An independent comparison of boron and 25 cross-sections, which does not depend on the thermal calibration, was made with 0.58 Mev neutrons by filling the boron chamber with an accurately measured amount of  $\text{BF}_3$  and comparing its geometry with the source and its counting rate to that of the fission sample which was used in the measurements of the 25 cross-section made at Wisconsin (Fig XVII-B-6, see A. O. Hanson CF-618). This measurement gave a value of 1.27 barns as indicated in Fig. 7. This may be compared to the value of 1.7 barns for 25. The boron value would be reduced to about 0.9 barns if the manganese flux measurements are assumed to be correct (see LA Handbook, LA-11).

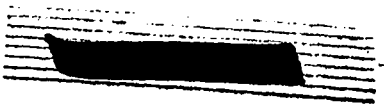
It might be worth pointing out that there was no evidence of any decrease in the pressure of the  $\text{BF}_3$  in the chamber over a period of 24 hours. The reason for this is that the chamber contained no organic materials. It was made with porcelain insulators and was sealed by lead gaskets.

#### Results of High Energy Comparison

The observed ratios of  $\sigma_B/\sigma_{25}$  are shown as a function of energy in Fig. 6. These ratios are normalized to a value of 6.0 for thermal energies which is based on the values  $\sigma_{25} = 645$  and  $\sigma_B = 708$  and  $\sigma_{B^{10}} = 3840$ . Relative values obtained with the gas chambers are normalized at a value of 1.43 at 0.29 Mev.

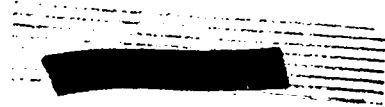
Using the values of the ratios from the curve in Fig. 6 and the values of the 25 cross-section given in the curve given in the LA Handbook (LA-11) we find the values for the  $B^{10}$  cross-section given in Fig. 7. The broken line is based on an extrapolation of the measurement of neutron flux by use of a long paraffin-covered fission counter.

-22-



The  $\sigma_B \cdot \sqrt{E}$  curve (Fig. 8) is interesting in that it shows clearly the resonance in the boron cross-section at about 0.25 Mev. An attempt was made to fit a resonance curve to the present data and hence get values for the boron cross-section in the region from 1 to 150 KV. But this attempt did not lead to any reliable conclusions.

The high value obtained for  $\sigma_B$  at 1.68 Mev cannot be regarded too seriously but it may indicate another resonance in the boron cross-section at a somewhat higher energy. Further measurements in this region are being planned for the near future.

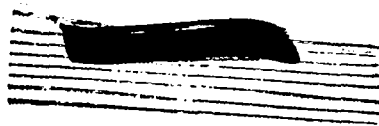


  
APPENDIXEXTENSION OF THE COMPARISON OF THE BORON AND 25 CROSS-SECTIONS FOR NEUTRONS  
OF ENERGIES UP TO 3.0 MEV.

Measurements of the relative cross-sections of boron and 25 have been made with neutrons having energies up to 3.0 Mev. The higher energy neutrons from the D-D source were made available for this purpose by the cooperation of Manley's group (P-3).

For this work the boron trifluoride chamber (Fig. 5) was lined with 5 mil gold foil. Manley's group had previously found that gold was effective in reducing the background count due to fast neutron reactions in the chamber walls. The chamber was filled to a pressure of 21 lbs. (gauge) of  $\text{BF}_3$  which gave a very high sensitivity and would make any remaining background relatively small. A very satisfactory plateau in the number of counts vs bias curve was obtained with thermal neutrons with a collecting voltage of 8000 volts. The plateaus obtained with high energy neutrons appeared approximately at the biases where they were expected but were not nearly as well defined. This was due to the fact that the chamber was more microphonic than it had been in the experiments reported above and the effective noise level was quite high when it was taken into the generator rooms. Also with the high energy neutrons the direct boron recoils raise the minimum bias at which a plateau could be observed. The plateaus, however, were sufficiently distinct to define the number of boron disintegrations to better than 10 percent. Probable statistical errors were in every measurement less than 3 percent so that the biggest uncertainty is in the interpretation of the bias curve.

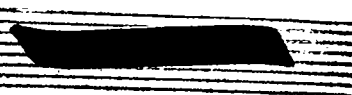
The fission detector used contained two foils, each carrying a deposit of about 1 milligram of material which contained about 72 percent of 25.



Corrections were made for the number of counts due to 28. The correction used at the 1.55 Mev point was 6 percent while the corrections at the higher energy points were all taken as 10 percent.

Measurements with the detector described above were taken at five neutron energies. Points at 1.08, 1.55, and 2.0 Mev were taken using neutrons from the Li (p,n) reaction supplied by the long electrostatic generator in W. The counting rates were taken with the boron and 25 chambers in the forward direction at distances of 5 and 2.5 inches from the target respectively. Both detectors were cadmium shielded. The same distances were used when the detectors were moved to the D-D source. Measurements at 2.5 and the 3.0 Mev were made by taking observations at 90° and 30° to the direction of the 200 Kev deuteron beam incident on a thick heavy ice target.

The results of the comparisons are shown in Figure 10. The value of the ratio of the counting rates at 1.08 Mev was used to normalize the ratios to that obtained previously (Fig. 6). It can be seen from Figure 10 that the ratio  $\sigma_B/\sigma_{25}$  has a very broad maximum at about 2.0 Mev but this could hardly be called a simple resonance. The extension of the  $\sigma_B$  curve was not made since the 25 cross-section is not known accurately in this region. The ratio plot gives the appearance of  $\sigma_B$  on the usual assumption that  $\sigma_{25}$  remains constant (1.6 barns) in this region. It was also not considered worthwhile to extend the  $\sigma_B \sqrt{E}$  curve since this quantity has no direct interpretation at these high energies.





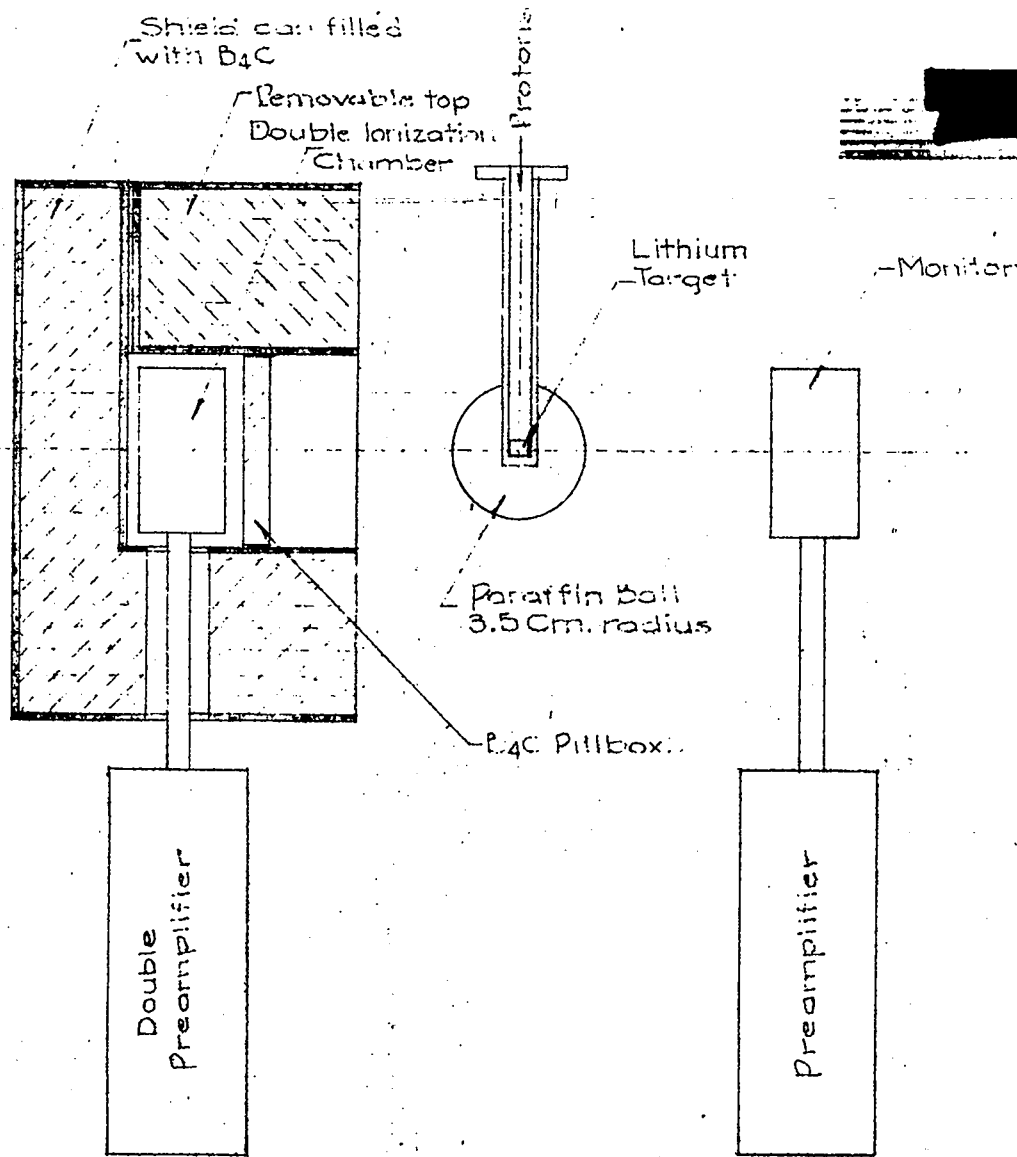


FIG. 1(a)-EXPERIMENTAL ARRANGEMENT

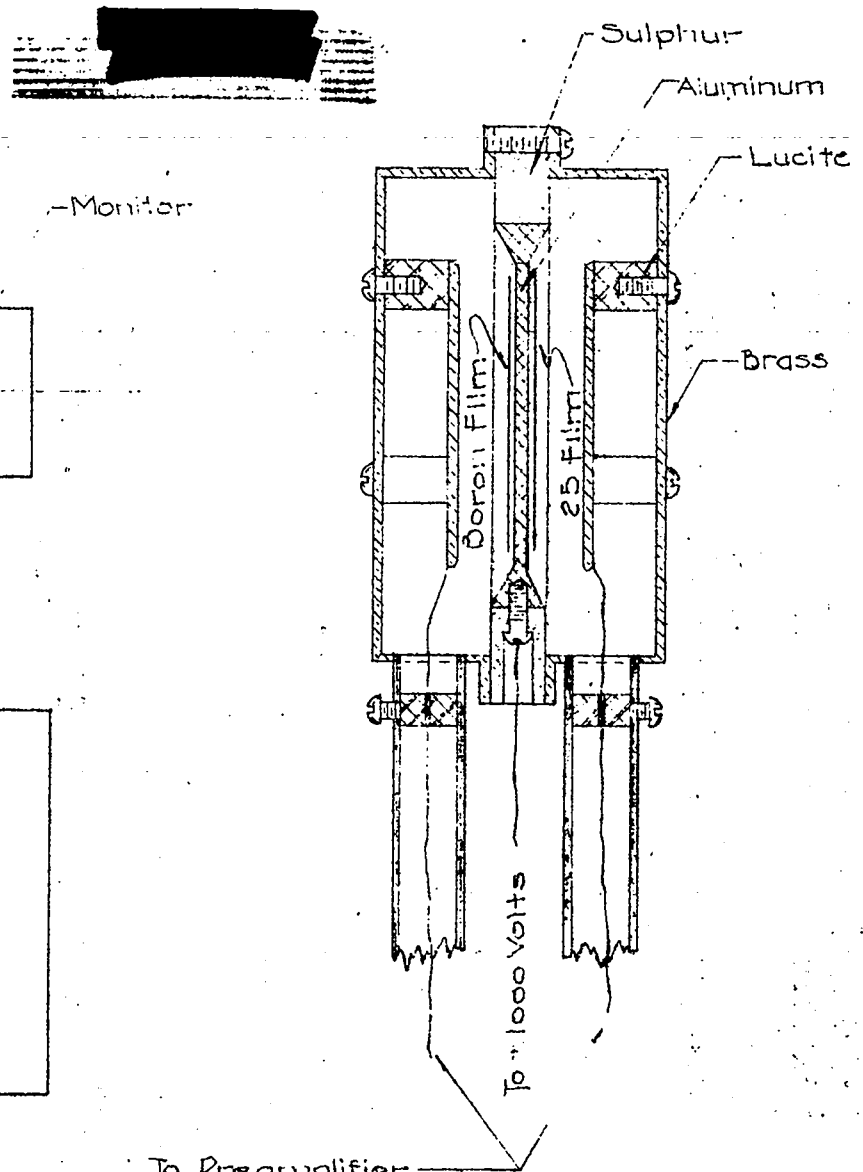


FIG. 1(b) DOUBLE IONIZATION CHAMBER  
ACTUAL SIZE

FIG. 2

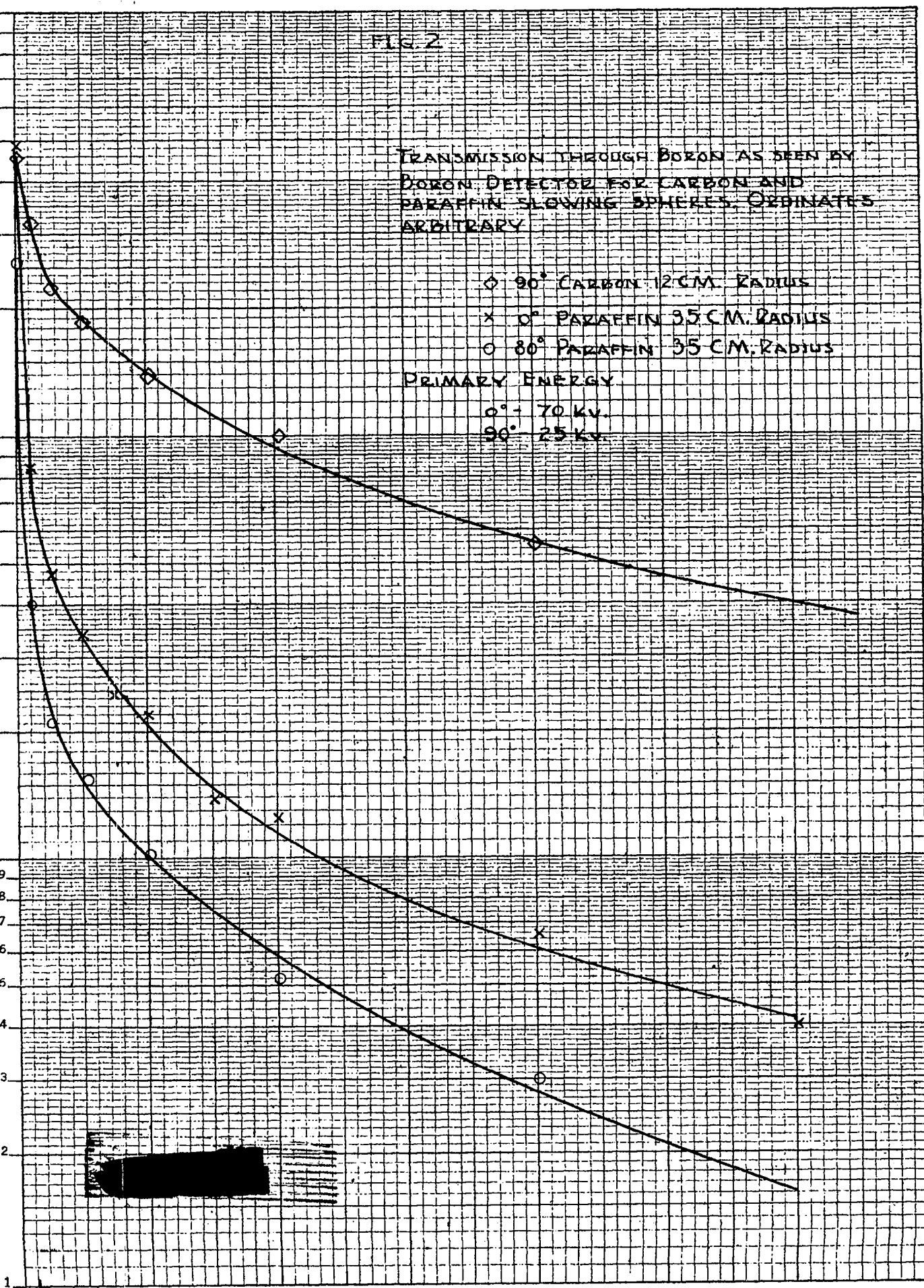
TRANSMISSION THROUGH BORON AS SEEN BY  
BORON DETECTOR FOR CARBON AND  
PARAFFIN SLOWING SPHERES. ORDINATES  
ARBITRARY

- ◇ 90° CARBON 12 CM. RADIUS
- × 0° PARAFFIN 35 CM. RADIUS
- 80° PARAFFIN 35 CM. RADIUS

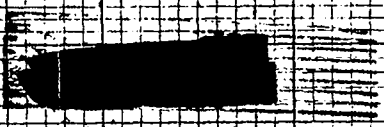
PRIMARY ENERGY

- 0° - 70 KV.
- 90° - 25 KV.

Intensity



KUFFEL & ESSER CO., N. Y. NO. 389 71  
Semi-Logarithmic, 3 Cycles X 10 to the Inch.  
MADE IN U.S.A.



(B<sub>4</sub>C) Boron Absorber GMS/CM (+ Cadmium)

APPROVED FOR PUBLIC RELEASE

APPROVED FOR PUBLIC RELEASE

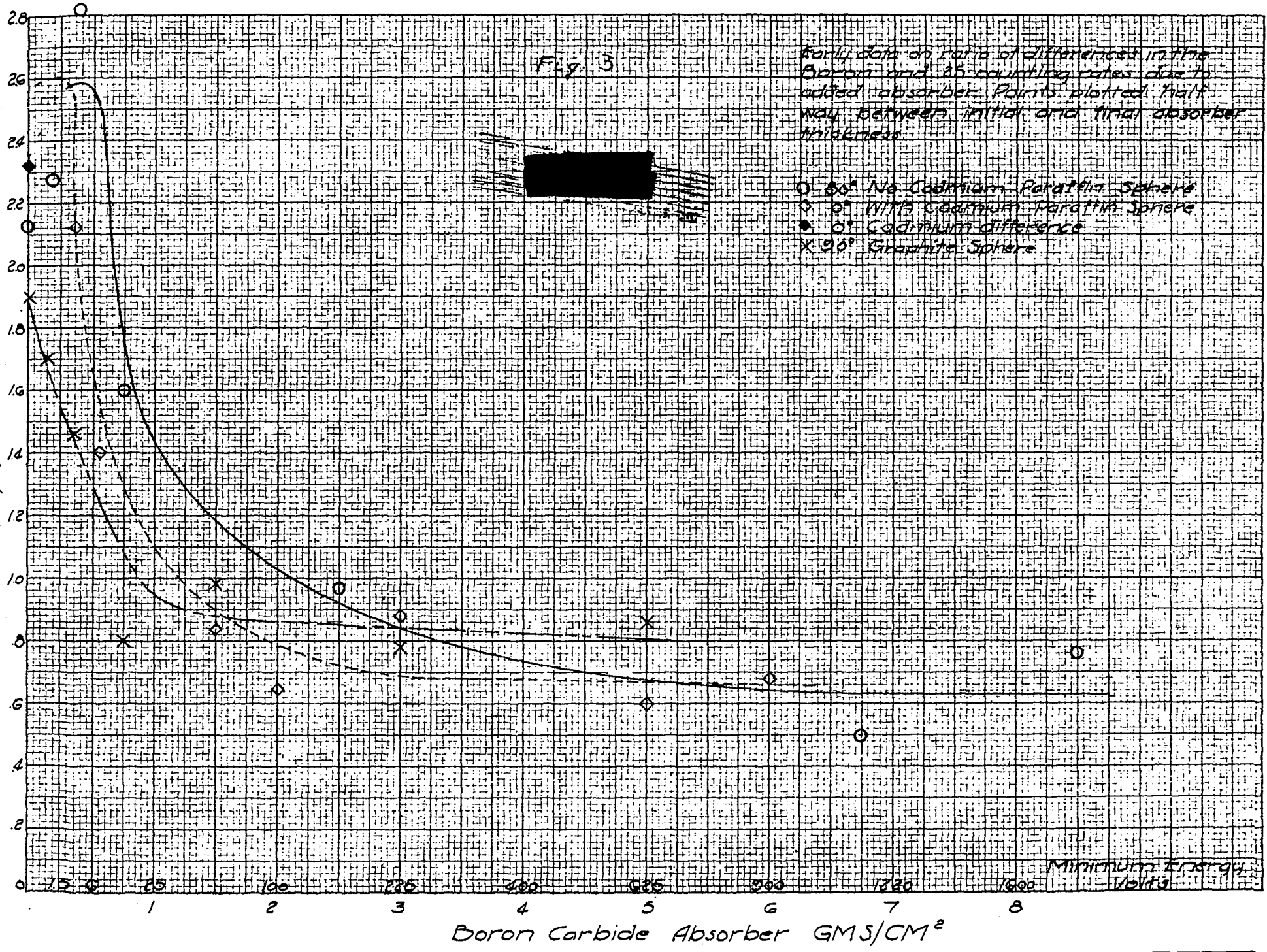
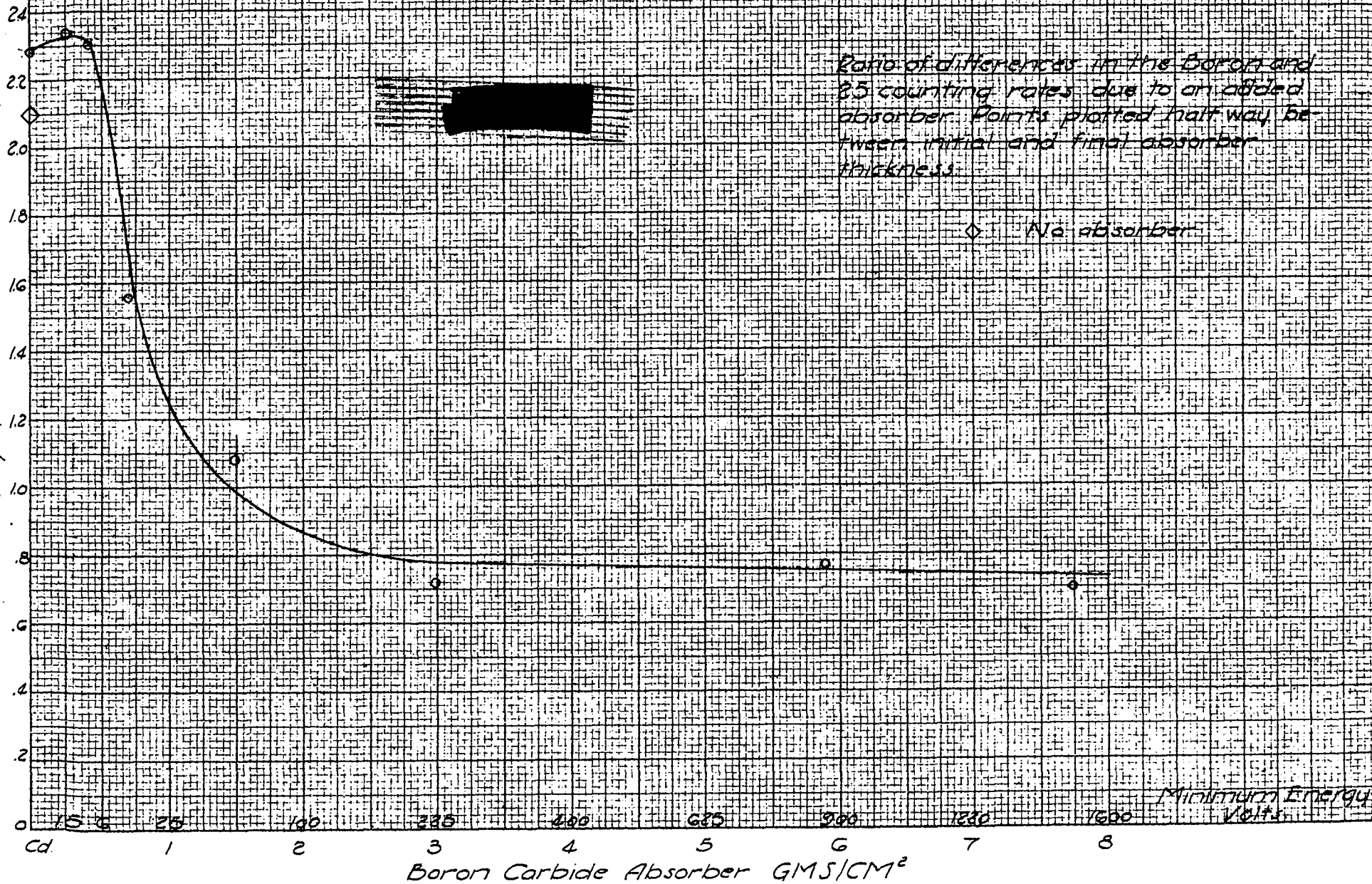


Fig. 4



APPROVED FOR PUBLIC RELEASE

APPROVED FOR PUBLIC RELEASE

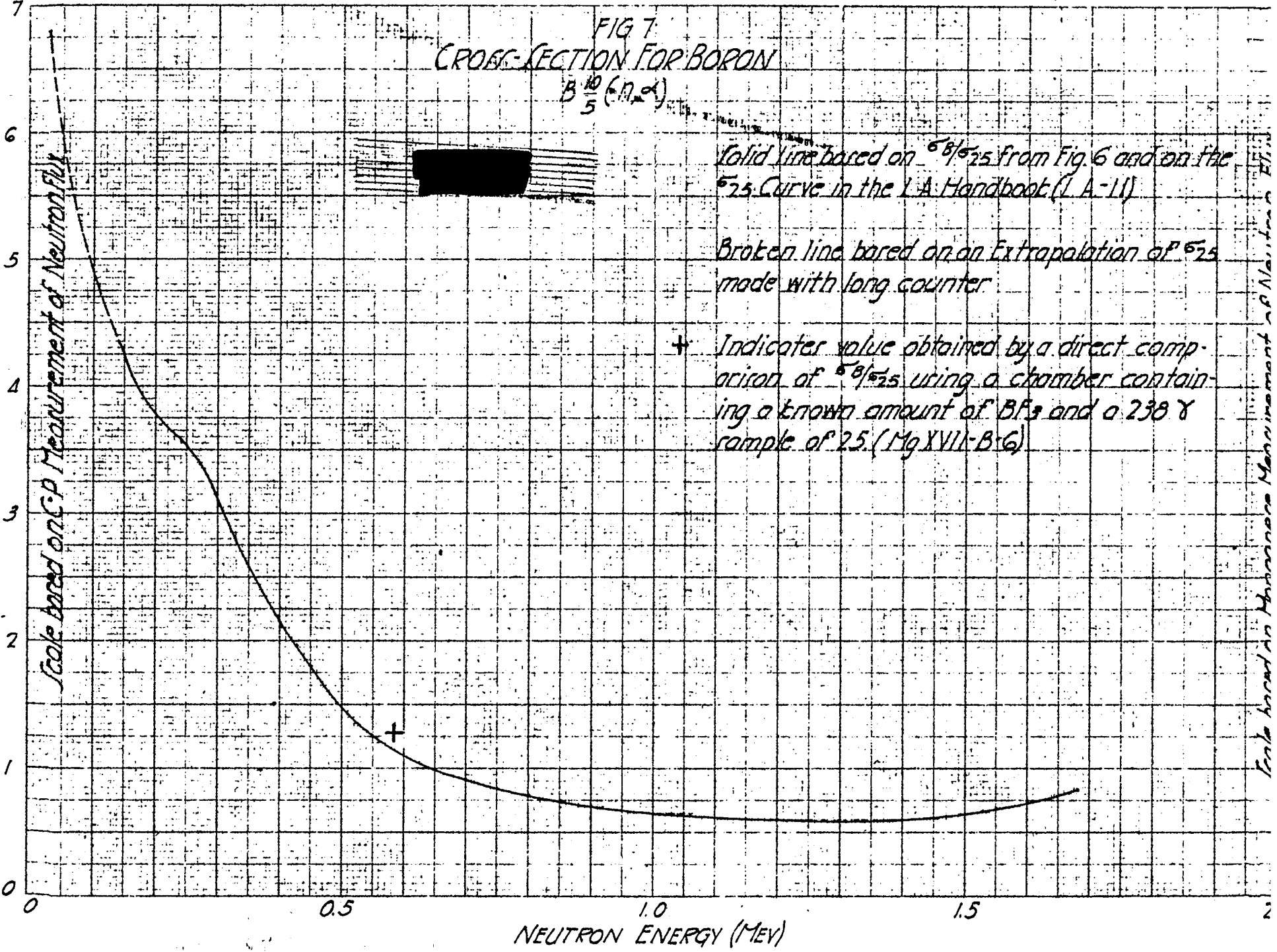






FIG 7  
CROSS-SECTION FOR BORON  
 $B^{10}(\alpha, n)$

Scale based on CP Measurement of Neutron Flux



Solid line based on  $^{60}\text{Co}$  from Fig. 6 and on the  $^{52}\text{Fe}$  Curve in the LA Handbook (LA-11)

Broken line based on an Extrapolation of  $^{52}\text{Fe}$  made with long counter

+ Indicator value obtained by a direct comparison of  $^{60}\text{Co}$  using a chamber containing a known amount of  $\text{BF}_3$  and a  $^{238}\text{U}$  sample of 25. (Mg XVII-B-6)

Fig. 7 contains information which is classified as CONFIDENTIAL

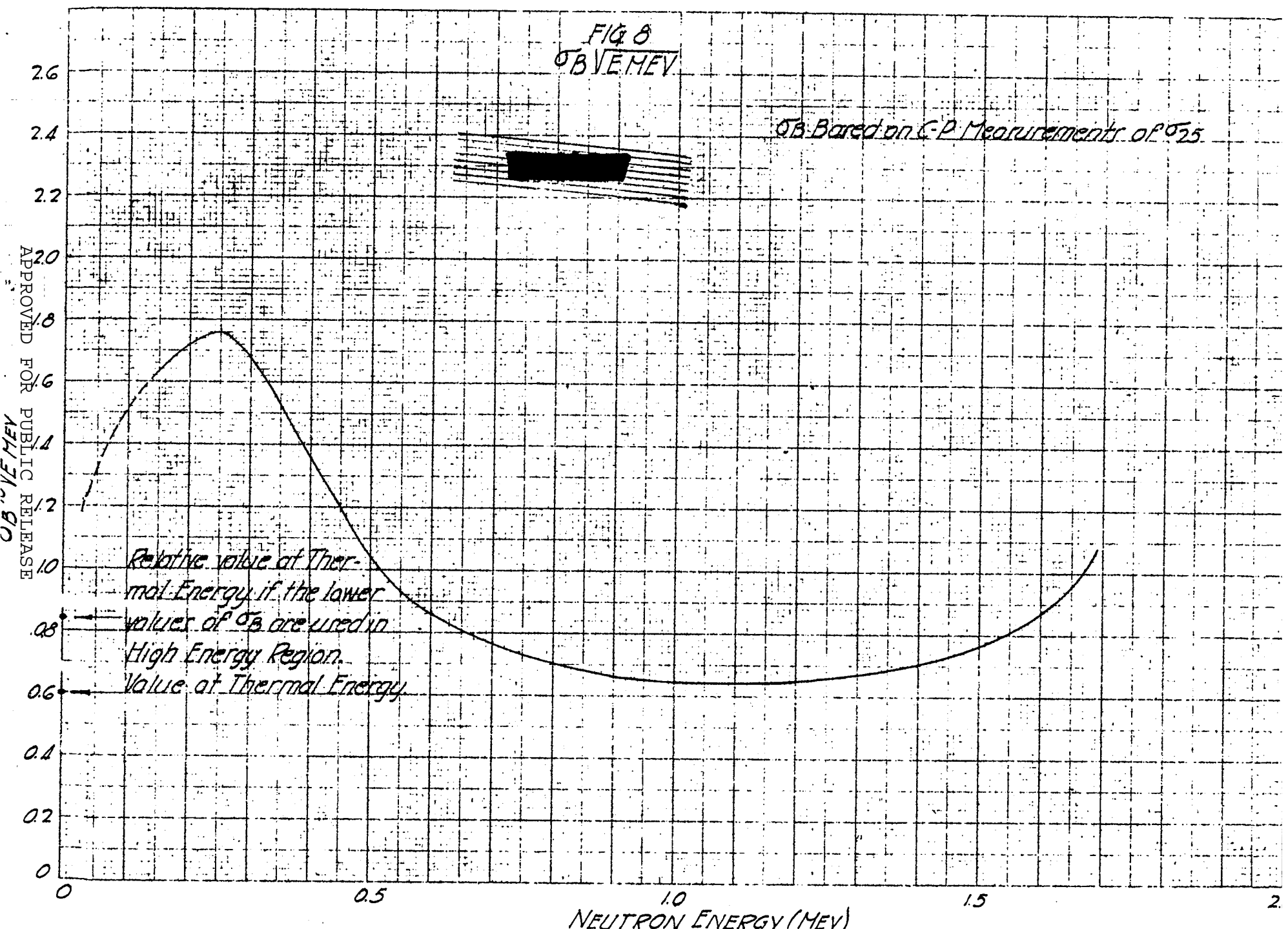




Fig. 9

$I$  = Neutrons per unit energy range from thick Li target  
 bombarded by 1.93 M.V. protons.  
 All other curves are in terms of activity in a 11v detector  
 per unit logarithmic energy range.  
 \* \* \* Computed from  $I$  for 3.5cm paraffin sphere.  
 o o o  $\sim I \delta B/\delta E$  derived from absorption curve for 80° data.  
 The histograms are described in the text.

APPROVED FOR PUBLIC RELEASE

APPROVED FOR PUBLIC RELEASE

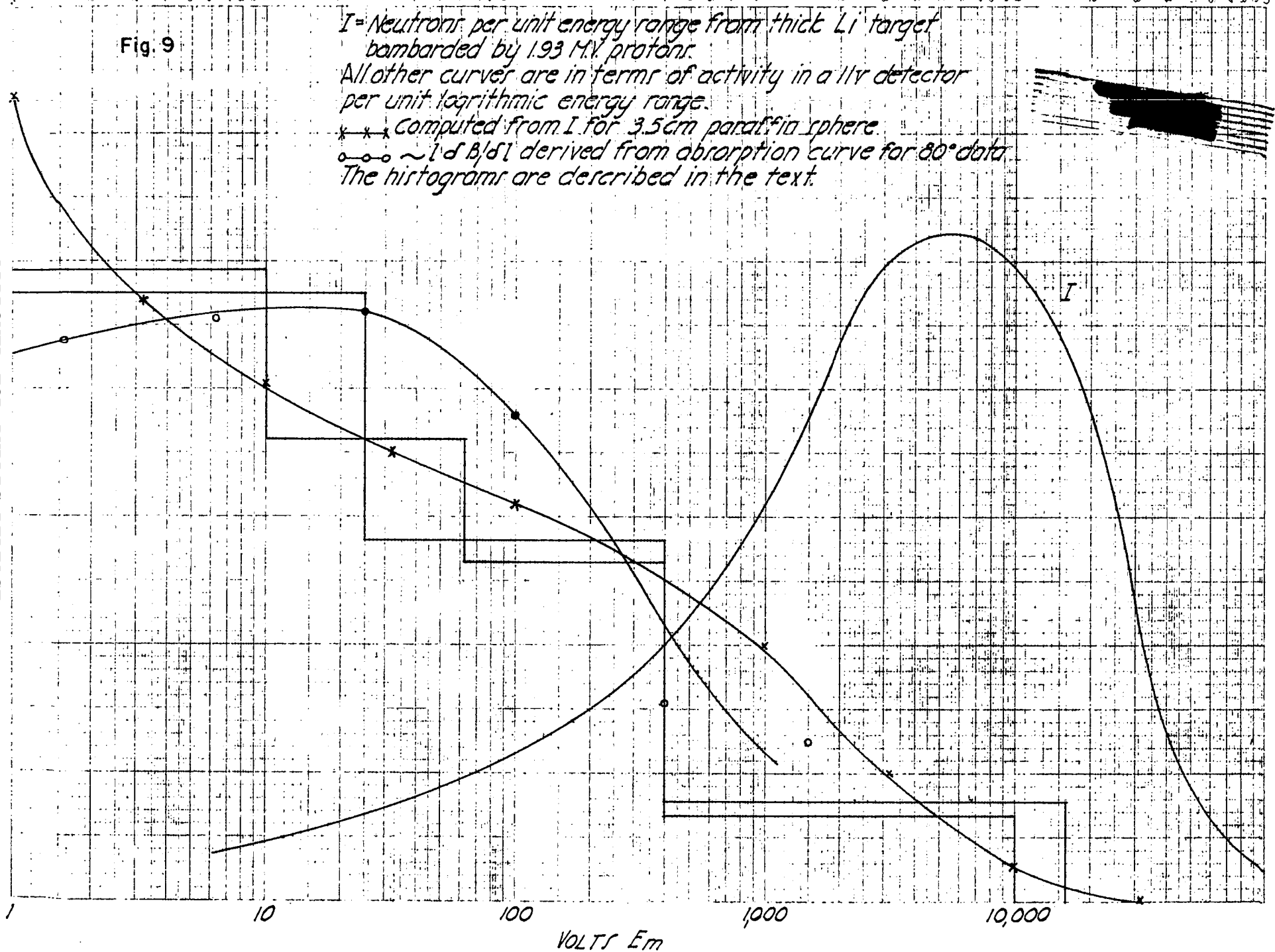
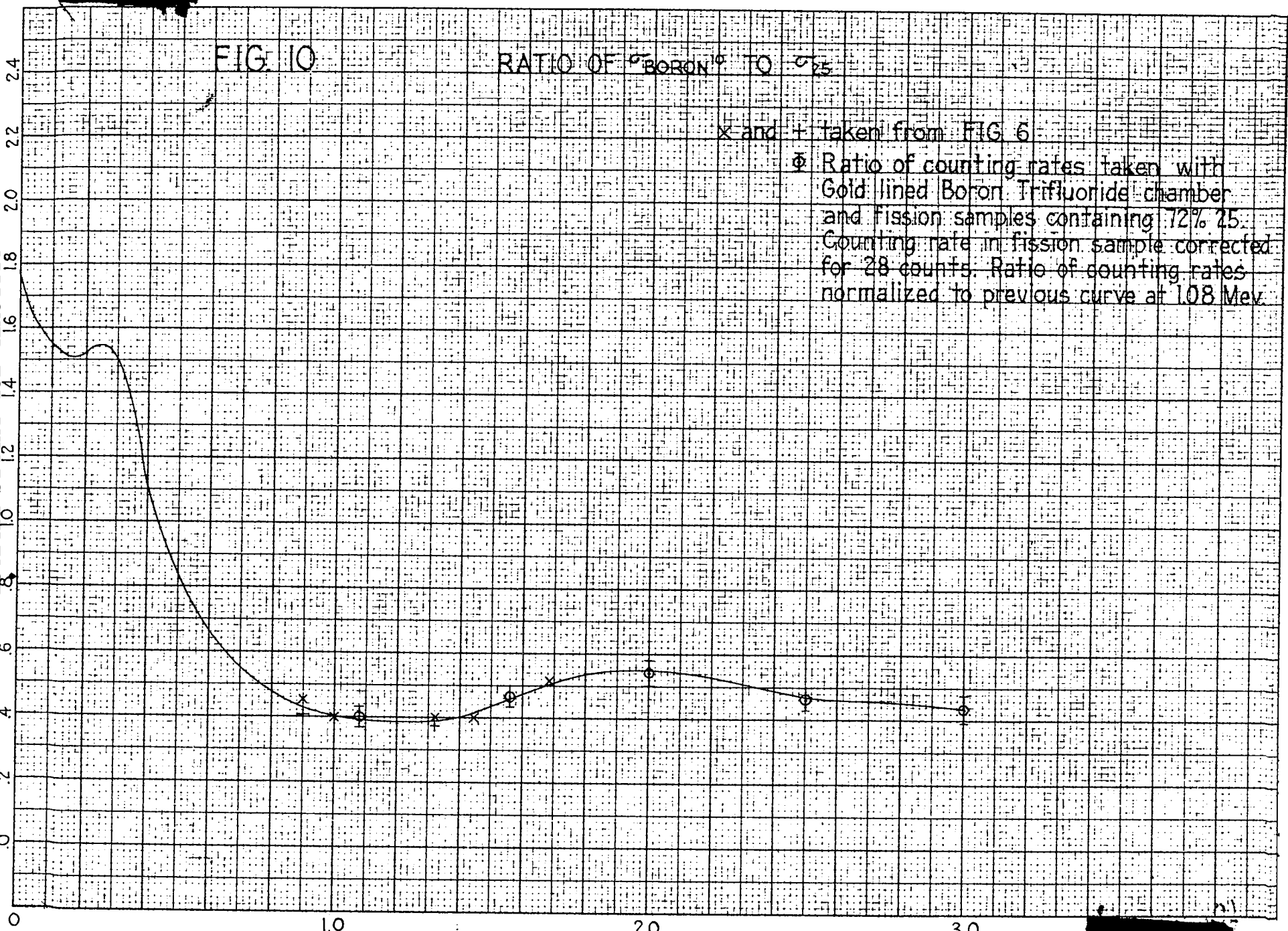


FIG. 10 RATIO OF  $^{10}\text{BORON}^0$  TO  $^{25}\text{S}$

x and + taken from FIG. 6  
⊙ Ratio of counting rates taken with Gold lined Boron Trifluoride chamber and fission samples containing 72%  $^{25}\text{S}$ . Counting rate in fission sample corrected for 28 counts. Ratio of counting rates normalized to previous curve at 1.08 Mev.

APPROVED FOR PUBLIC RELEASE  
9/10/59

APPROVED FOR PUBLIC RELEASE



Neutron Energy (Mev)

